

Modeling Activity and Target-Dependent Developmental Cell Death of Mouse Retinal Ganglion Cells *Ex Vivo*

Sylvie Voyatzis^{1,2,3}, Aude Muzerelle^{1,2,3}, Patricia Gaspar^{1,2,3}, Xavier Nicol^{1,2,3,*}

1 Institut National de la Santé et de la Recherche Médicale, Unité mixte de Recherche en Santé 839, Paris, France, **2** Université Pierre et Marie Curie, Paris, France, **3** Institut du Fer à Moulin, Paris, France

Abstract

Programmed cell death is widespread during the development of the central nervous system and serves multiple purposes including the establishment of neural connections. In the mouse retina a substantial reduction of retinal ganglion cells (RGCs) occurs during the first postnatal week, coinciding with the formation of retinotopic maps in the superior colliculus (SC). We previously established a retino-collicular culture preparation which recapitulates the progressive topographic ordering of RGC projections during early post-natal life. Here, we questioned whether this model could also be suitable to examine the mechanisms underlying developmental cell death of RGCs. Brn3a was used as a marker of the RGCs. A developmental decline in the number of Brn3a-immunolabelled neurons was found in the retinal explant with a timing that paralleled that observed *in vivo*. In contrast, the density of photoreceptors or of starburst amacrine cells increased, mimicking the evolution of these cell populations *in vivo*. Blockade of neural activity with tetrodotoxin increased the number of surviving Brn3a-labelled neurons in the retinal explant, as did the increase in target availability when one retinal explant was confronted with 2 or 4 collicular slices. Thus, this *ex vivo* model reproduces the developmental reduction of RGCs and recapitulates its regulation by neural activity and target availability. It therefore offers a simple way to analyze developmental cell death in this classic system. Using this model, we show that ephrin-A signaling does not participate to the regulation of the Brn3a population size in the retina, indicating that ephrin-A-mediated elimination of exuberant projections does not involve developmental cell death.

Citation: Voyatzis S, Muzerelle A, Gaspar P, Nicol X (2012) Modeling Activity and Target-Dependent Developmental Cell Death of Mouse Retinal Ganglion Cells *Ex Vivo*. PLoS ONE 7(2): e31105. doi:10.1371/journal.pone.0031105

Editor: Harold A. Burgess, National Institutes of Health/NICHHD, United States of America

Received: September 22, 2011; **Accepted:** January 2, 2012; **Published:** February 17, 2012

Copyright: © 2012 Voyatzis et al. This is an open-access article distributed under the terms of the Creative Commons Attribution License, which permits unrestricted use, distribution, and reproduction in any medium, provided the original author and source are credited.

Funding: This work was supported by a grant from Fondation Internationale pour la Recherche en Paraplégie to PG, a Region Ile de France fellowship to SV, an IOF Marie Curie fellowship to XN, and by Institut National de la Santé et de la Recherche Médicale and Université Pierre et Marie Curie. The funders had no role in study design, data collection and analysis, decision to publish, or preparation of the manuscript.

Competing Interests: The authors have declared that no competing interests exist.

* E-mail: xavier.nicol@inserm.fr

‡ Current address: Institut de la Vision, Institut National de la Santé et de la Recherche Médicale, Unité mixte de Recherche en Santé 968, Paris, France

Introduction

During the development of the central nervous system, neurogenesis and programmed cell death occur concomitantly. Developmental cell death plays different roles in morphogenesis: regulation of the size of progenitor population in the CNS, removal of damaged cells, optimization of cell population matching between interconnected neurons and removal of neurons with ectopic connections [1]. In the mouse retina, the main wave of histogenetic cell death occurs during the first two postnatal weeks, coinciding with the formation of retinotopic maps in the superior colliculus (SC). All retinal cell types undergo developmental cell death, with different time-courses [2,3] but retinal ganglion cells (RGCs) are the ones undergoing substantial developmental cell death. While 5% of the photoreceptors undergo developmental cell death, up to 50% of RGCs are lost due to cell death, peaking between P2 and P4 in mice [3,4]. However, the methods used to quantify the reduction in RGC number have often been indirect, and have led to a large variability in the results, ranging from 9% [3] to 90% [5].

The size of the RGC population is dependent on electrical activity [6] and is regulated by competition for trophic factors between retinal axons in their targets [7–10]. The reduction of

RGC number participates in the elimination of subpopulations of ectopically projecting RGCs [11,12]. In the adult, RGC axons are topographically organized in their targets, with the temporo-nasal axis of the retina projecting on the rostro-caudal axis of the SC [13,14]. Temporal axons first overshoot their final arborization zone in the rostral part of the SC, reaching the caudal SC. Topography is subsequently refined during the first post-natal week in mice by eliminating exuberant projections [15–17]. Blocking electrical activity in the retina promotes the survival of the ectopically projecting temporal RGCs [18,19]. Similar mechanisms were found to operate for the establishment of bilateral retinal projections: most of the RGCs project contralaterally [20] and lack of neural activity maintains RGCs projecting to the ipsilateral SC that are normally eliminated [11]. However, it remains unclear whether developmental cell death has a role in the elimination of all populations of ectopically projecting RGCs.

Specific molecular markers that are expressed in a large population of RGCs are now available. Such markers allow a direct estimation of RGC number. For instance the POU domain transcription factor Brn3a labels a large population of RGCs. The Brn3a RGCs were shown to contribute only to the principal retino-thalamic and retino-collicular visual pathways and to be excluded from the subcortical pathways of the accessory optic

system, moreover they project mainly contralaterally [21]. We used this marker to evaluate the number of RGCs in the retina at several time-points during the first postnatal week in mice. We analyzed a previously established *ex vivo* retino-collicular co-culture mimicking the development of neuronal network between the retina and the SC [22]. We show that the time course of the reduction of RGC number is similar to that occurring *in vivo*. In this co-culture, electrical activity regulates the size of the RGC population, mimicking *in vivo* observations. Similarly, manipulation of the target size enabled an evaluation of the influence of competition for space between retinal axons on RGC survival. We used this model to assess the influence of ephrin-As and the topographic organization of the retino-collicular projections on the population size of a genetically defined population of RGCs.

Results

Reduction of the number of Brn3a-expressing RGCs between P0 and P7

Brn3a expression is limited to post-migratory RGCs, beginning at E12.5 with a stable expression until adulthood [21]. To estimate changes in Brn3a-expressing RGC number during the period of developmental cell death, we immunostained serial sections of P0, P3 and P7 retinas for Brn3a, and estimated the total number of Brn3a RGCs in the retina. Between P0 and P7, the population of Brn3a-positive cells in the retina decreased by ~48% (Fig. 1A and 1B). Concurrently with the decline of Brn3a-expressing RGC, retinal surface increased, and, the RGC layer of the retina reorganized into a single cell layer (Fig. 1A).

To evaluate whether reduction in cell number was a general feature of all retinal cell types during the first post-natal week, retinal sections were stained for recoverin, a marker for photoreceptors [23], or choline acetyltransferase (ChAT), a marker for starburst amacrine cells [24,25], a subpopulation of interneurons in the inner nuclear layer. Between P0 and P7 both recoverin- and ChAT-positive cell populations expanded (Fig. 2A and 2B). Thus, the reduction in the number of Brn3a-positive RGCs during the first postnatal week does not reflect a general loss of all retinal cell types. The observed timing of reduction of Brn3a-positive RGCs coincides with the period of maximal developmental cell death of RGCs described in rodents [3] and falls within the range of previous numerical estimates (9 to 90% [3,5,26–28]).

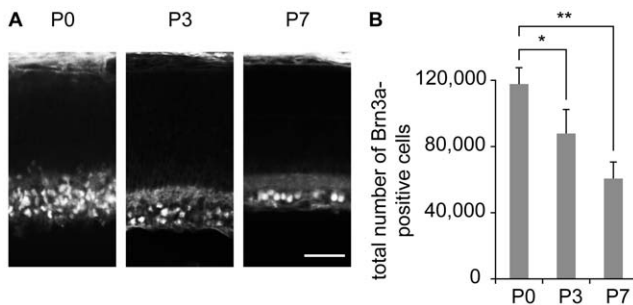


Figure 1. The number of Brn3a-expressing RGCs undergoes a reduction during the first postnatal week. (A) P0, P3, and P7 retinal sections were immunostained with a Brn3a antibody. The inner surface of the retina (RGC layer) is down. The density of Brn3a-expressing cells decreases from P0 to P7 and the retinal ganglion cell layer reorganizes from a multiple cell layer at P0 to a single cell layer at P7. (B) The total number of Brn3a-positive RGCs in the retina declines between P0 and P7. n≥3 for each age. Error bar, s.e.m.; scale bar 50 μm; * p<0.05, ** p<0.01, Kruskal-Wallis test. doi:10.1371/journal.pone.0031105.g001

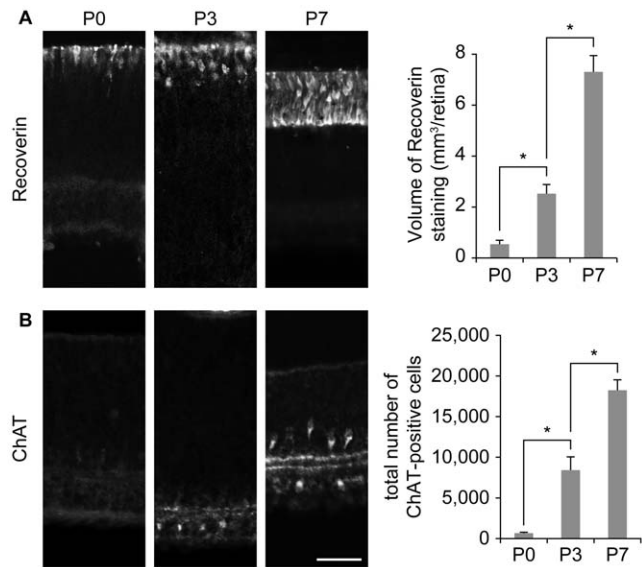


Figure 2. The number of photoreceptors and starburst amacrine cells increases during the first postnatal week. (A) Recoverin and (B) ChAT immunoreactivity reveals photoreceptors and starburst amacrine cells respectively. Both cell types undergo an expansion of their population between P0 and P7. n≥3 for each age. Error bar, s.e.m.; scale bar 50 μm; * p<0.05, Kruskal-Wallis test. doi:10.1371/journal.pone.0031105.g002

Reduction of RGC number is mimicked in a retino-collicular co-culture

We examined the maturation of these retinal cell types in an *ex vivo* model which combines an E15.5 retinal explant and a parasagittal slice of SC, one of the targets of Brn3a RGCs (Fig. 3A) [22]. The preparation was fixed, immunostained for Brn3a and counterstained with bisbenzimidazole to identify the pyknotic profiles of dying cells after 4, 7, 12 or 21 days *in vitro* (equivalent to P0, P3, P7 and P12 respectively for the age of the retinal explant). We observed a ~68% decrease in the density of the Brn3a positive neurons from DIV4 to DIV7, and a further ~22% decrease in the density from DIV7 to DIV12 (Fig. 3B and 3C). The initial reduction of Brn3a-positive RGCs coincided with a high number of pyknotic profiles (Fig. 3D and 3E), indicating that a large amount of cells are undergoing cell death. No significant change in RGC number was observed between DIV12 to DIV21 indicating a long term survival of RGCs after the initial massive loss (Fig. 3C). There was also a gradual histotypic organization of the Brn3a-positive cells that became organized in a layer generally at the periphery of the retinal explant and to a lesser extent in the center of the explant (Fig. 3B). This elimination of Brn3a-positive cells is therefore similar to the reorganization of RGCs *in vivo* between P0 and P7 that leads to the formation of a single cell layer (Fig. 1A). Retinal explants from mouse reporter lines expressing GFP under the control of the β-actin promoter [29] or β-galactosidase under the control of the Brn3a promoter [30] were used to verify that RGC axons were invading the superior colliculus *ex vivo*. In both conditions, GFP-positive or LacZ-positive axons were found in the collicular slice at DIV12, invading specifically the superficial layers of the SC (Figure 3F and 3G) as previously described [19,22]. To ensure that the collicular slice was still alive at the end of the *in vitro* period, extracellular electrophysiological recordings of the mesencephalic slice were performed. Large bursts of spontaneous correlated activity were detected, confirming the viability of the collicular slice during the entire culture period (Figure 3H).

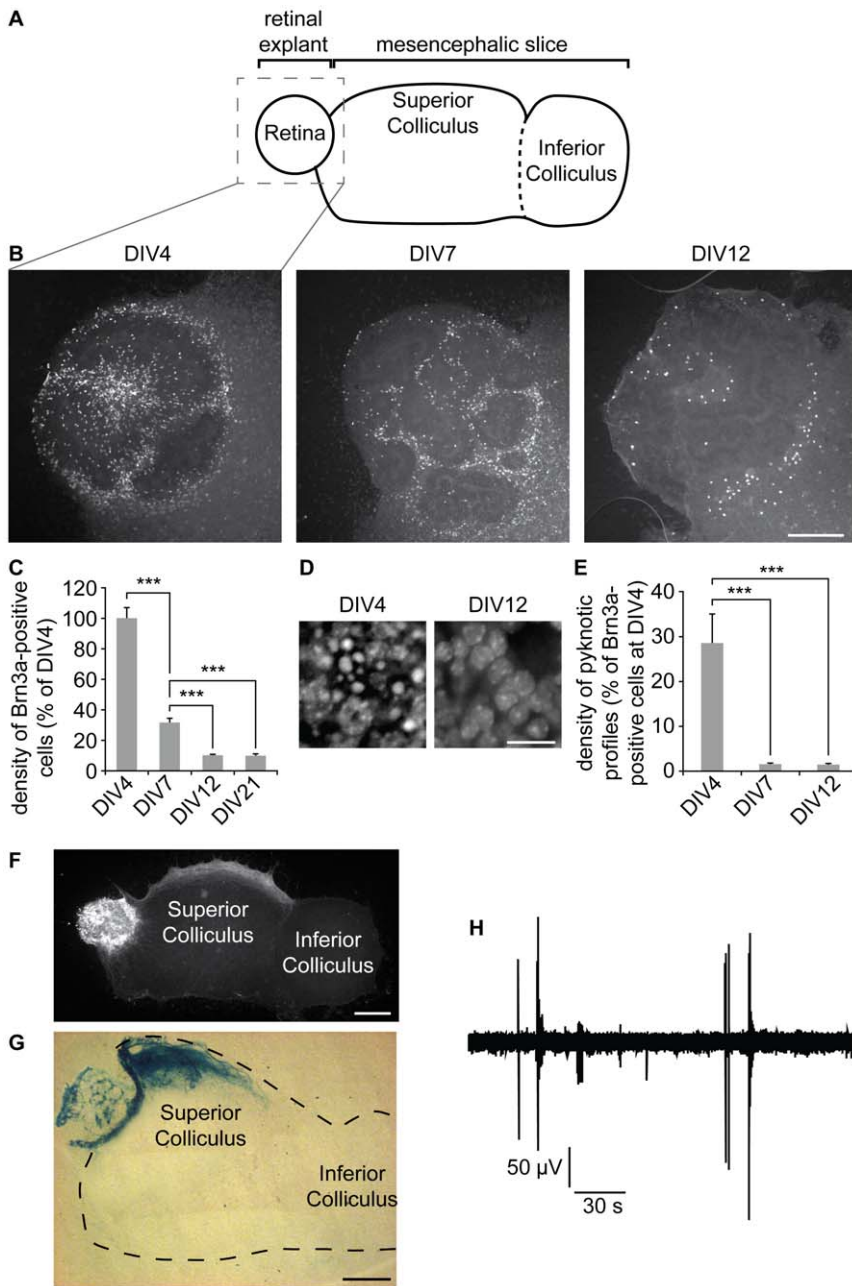


Figure 3. The number of Brn3a-expressing cells in retino-collicular co-cultures decreases between DIV4 and DIV12. (A) Schematic of the retino-collicular co-culture. A retinal explant is placed in contact with the rostral end of a parasagittal mesencephalic slice containing the SC. (B, C) The density of cells immunoreactive for Brn3a undergoes a reduction of ~68% between DIV4 and DIV7, and a further decrease of ~22% between DIV 7 and DIV12. No further reduction is observed between DIV12 and DIV21. The density measured for each age was normalized to the density of Brn3a-positive cells at 4DIV. (D, E) Density of dying cells revealed by the number of bisbenzimidazole-stained pyknotic profiles, and measured at DIV4, DIV7 and DIV12. The density of pyknotic profiles was normalized to the density of Brn3a-positive cells at DIV4 to coarsely estimate the percentage RGCs lost at each age. This estimation would only give an order of magnitude of the percentage of dying Brn3a-positive RGCs because only ~30% of RGCs express Brn3a and other cell types are present in the retinal explant. (F) Axons from GFP expressing retinal explants invade the superficial layers of the SC at DIV12. (G) Projections from Brn3a-positive RGCs are detected in the SC using a retinal explant from a Brn3a-LacZ reporter mouse line. (H) Field electrophysiological recording of the collicular slice at DIV12. Large bursts of spontaneous correlated activity are detected. B, scale bar 200 μ m. D, scale bar 50 μ m. F,G, scale bar 500 μ m. Error bar, s.e.m.; $n \geq 10$ cultures per condition; *** $p < 0.001$, ANOVA. doi:10.1371/journal.pone.0031105.g003

We evaluated the evolution of photoreceptors and starburst amacrine cells in the retino-collicular *ex vivo* model, by immunostaining the cultures for recoverin or ChAT respectively. The density of photoreceptors increased between DIV4 and DIV12, and their organization in the retinal explant switched from a

uniform distribution to enrichment within the center of the explants (Fig. 4A). Few starburst amacrine cells were detected at DIV4 and their number increased progressively at DIV7 and DIV12. At DIV12, starburst amacrine cells were located between the RGCs and the photoreceptors, a position similar to that observed

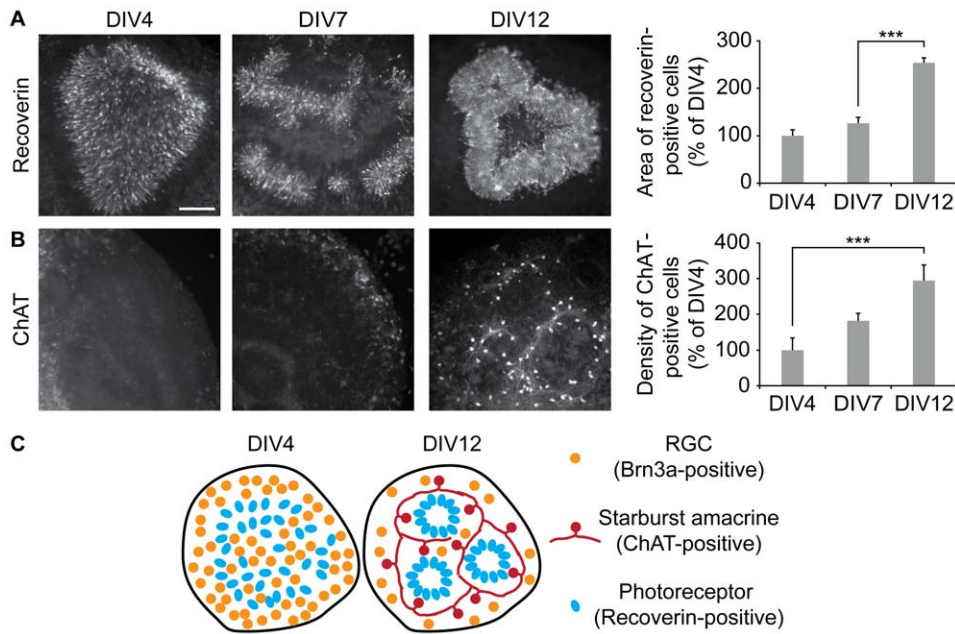


Figure 4. Photoreceptor and starburst amacrine cell populations expand in the retino-collicular co-cultures between DIV4 and DIV12. (A) Recoverin and (B) ChAT immunoreactivity reveals photoreceptors and starburst amacrine cells respectively in the retinal explant of retino-collicular co-cultures. Both cell types undergo an expansion between DIV4 and DIV12. Scale bar 100 μ m; Error bar, s.e.m.; $n \geq 7$ cultures per condition; *** $p < 0.001$, ANOVA. (C) Reorganization of the retinal explant *ex vivo*. At DIV4, RGCs (orange) and photoreceptors (blue) are mixed in the explant. After 12 days *in vitro*, RGCs are preferentially located at the border of the retinal explant, while photoreceptors form rosette-like structures in the center of the explant. ChAT amacrine cells (red) are positioned between RGCs and photoreceptors. doi:10.1371/journal.pone.0031105.g004

in vivo (Fig. 4B). The expansion of the recoverin- and ChAT-positive population size shows that there is ongoing cell division in the retinal explant.

Overall, this analysis showed that the development of the retinal explant in the retino-collicular co-culture system follows the histotypic reorganization of the retina *in vivo*, and mimics the reduction of RGC number that occurs during the first post-natal week (Fig. 4C).

Reduction in RGC number is activity-dependent

One of the proposed functions for RGC selective death is to complement the topographic refinement of the retinotopic map that is initially coarsely organized in the rodent SC, particularly across the rostro-caudal dimension [16]. The refinement of retino-collicular maps is dependent on electrical activity of RGCs [31] and can be partially explained by the activity-dependent preferential cell death of RGCs that overshoot their termination zone [11,12]. However, the influence of electrical activity on the total number of RGCs is largely unknown. We have previously demonstrated that the rostro-caudal refinement of the topography is reproduced in the retino-collicular slice preparation [22] and that the sodium channel blocker tetrodotoxin (TTX) causes retinal axons to maintain exuberant axons in inappropriate targets [19] (Fig. 5A). We evaluated the regulation of Brn3a-positive RGC number, in retino-collicular co-cultures in which TTX was used to block neuronal activity during the entire culture period. TTX treatment induced a ~64% increase in the number of Brn3a-positive cells at DIV12 compared to control cultures (Fig. 5B and 5C). We conclude that neural activity contributes to the elimination of Brn3a-positive RGCs.

RGC number reduction is dependent on target availability

Competition for target availability and neurotrophic factors regulates survival of RGCs as shown in monocular deprivation or

partial collicular ablation experiments [7–11,32]. However testing this hypothesis by increasing the size of the target has not been possible *in vivo*. The retino-collicular co-culture model enabled the manipulation of the target size, by varying the number of collicular slices in contact with the retinal explant (Fig. 6A). Doubling the target size reduced the loss of Brn3a-positive cells at DIV12 and multiplying the target size by 4 led to a further reduction of cell death (Fig. 6B). Increasing the number of mesencephalic slices that faced a single retinal explant did not modify the pattern of retinal projections in each superior colliculus (Fig. 6C). This suggests that retinal axons compete for space in the SC, and that one of the results of this competition is the elimination of Brn3a-positive RGCs.

Ephrin-A-induced retinocollicular topography does not influence RGC number reduction

In addition to being regulated by electrical activity and competition for target availability, connectivity between the retina and its target is modulated by ephrin-A-dependent axonal repulsion [33]. Topography of retinal projections is dependent on ephrin-As *in vivo* [33]. Ephrin-A signaling regulates apoptosis of neuronal progenitors in the cerebral cortex [34], but its involvement in the regulation of the RGC population size is unclear. To evaluate the involvement of ephrin-As in the regulation of RGC number, we activated all EphA receptors in the retino-collicular co-cultures with ephrin-A5 incubation from DIV1 to DIV12. We have previously showed that this treatment prevented the development of the topography in the *ex vivo* retino-collicular system [22] (Fig. 7A). In contrast however, ephrin-A5 treatment did not affect the number of Brn3a-positive cells in the retinal explant at DIV12 (Fig. 7B and 7C), demonstrating that ephrin-A signaling does not influence the number of Brn3a-expressing RGCs, and

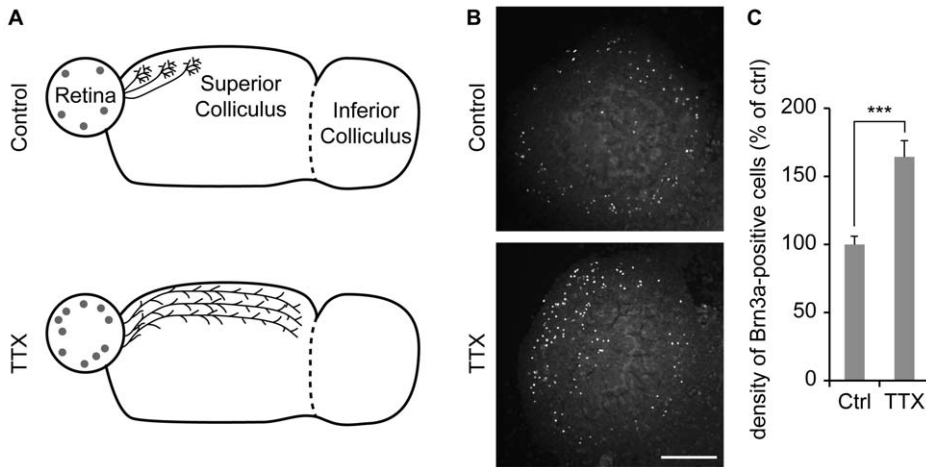


Figure 5. Blockade of electrical activity limits the reduction in the number of Brn3a-expressing cells. (A) TTX treatment prevents the retinotopic organization of axonal arbors *ex vivo*. Temporal axons arborize in the rostral SC in control conditions. In contrast, electrical activity blockade with TTX abolishes the preference of axons from the temporal retina for the anterior SC as described in [19]. Grey circles symbolize Brn3a-positive RGCs and their density is representative of the number of Brn3a-labeled cells in each condition. (B) Incubation of retino-collicular co-cultures in the sodium channel blocker TTX increases the number of Brn3a-immunoreactive cells in retinal explants at DIV12. (C) TTX treatment causes a ~64% increase in the number of Brn3a-expressing cells at DIV12. Error bar, s.e.m.; Scale bar 200 μ m; $n \geq 22$ cultures per condition; *** $p < 0.001$, ANOVA. doi:10.1371/journal.pone.0031105.g005

suggesting that topographic errors do not influence the elimination of RGCs.

Discussion

Direct estimation of RGC loss during the first postnatal week

We monitored the development of Brn3a-expressing RGCs during the first postnatal week. Brn3a is a marker of a subpopulation of RGCs with specific projections to the thalamus and colliculus [21]. Our direct measurements *in vivo* approximate the amount of RGC loss between P0 and P7 to ~48%, which falls within the large range

of previous approximations and refines the previous estimations performed using indirect methods [3,5,26–28]. This included the quantification of pyknotic profiles in the inner nuclear layer (RGC layer) [3] which can overestimate cell death as it does not allow to distinguish RGCs from displaced amacrine cells, that account for 50% of the cells in the RGC layer [35,36]. In contrast, retrograde labeling using tracer injections [27] is highly dependent on the size of the injection and may underestimate cell death. The comparison of the number of axons in the optic nerve with the number of cells in the RGC layer [28] is also affected by the presence of amacrine cells that are present in the RGC layer. This method also assumes that all RGC axons have a single branch in the optic nerve.

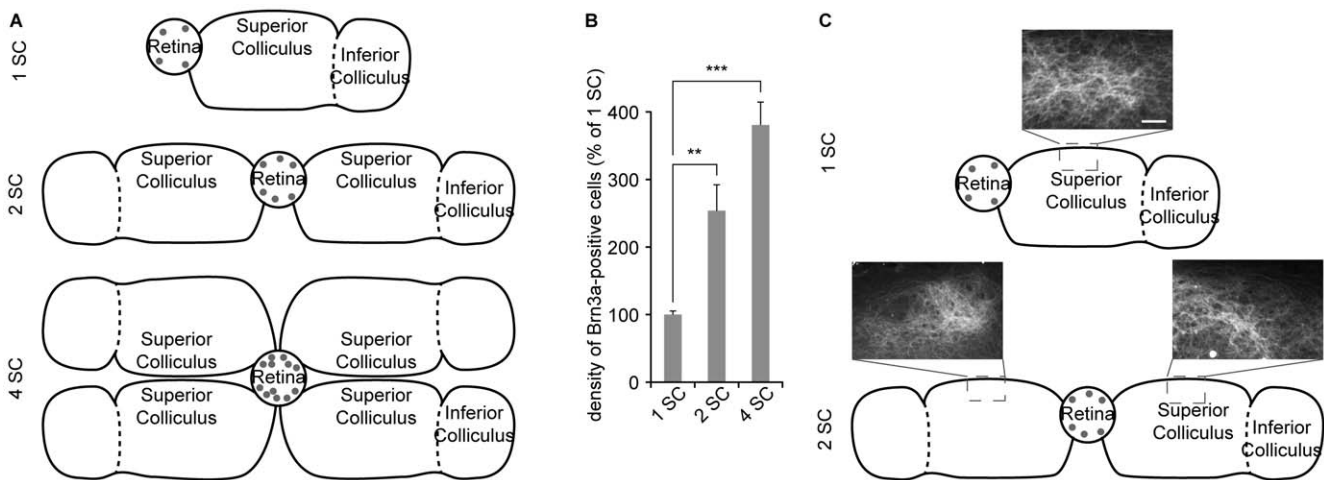


Figure 6. Increasing the size of the target reduces the elimination of Brn3a-expressing cells. (A) The modulation of target availability was achieved by increasing the number of mesencephalic slices in contact with the retinal explant. Grey circles symbolize Brn3a-positive RGCs and their density is representative of the number of Brn3a-labeled cells in each condition. (B) The density of Brn3a-immunoreactive cells in retinal explants confronted with 2 (2 SC) or 4 (4 SC) collicular slices was increased by ~153% and ~280% respectively at DIV12 in comparison with parallel cultures with a single collicular slice. (C) Axonal arbors from GFP-expressing retinas are detected in the superior colliculus of all mesencephalic slices that are available to them. Error bar, s.e.m.; Scale bar 50 μ m; $n \geq 10$ cultures per condition; ** $p < 0.01$, *** $p < 0.001$, ANOVA. doi:10.1371/journal.pone.0031105.g006

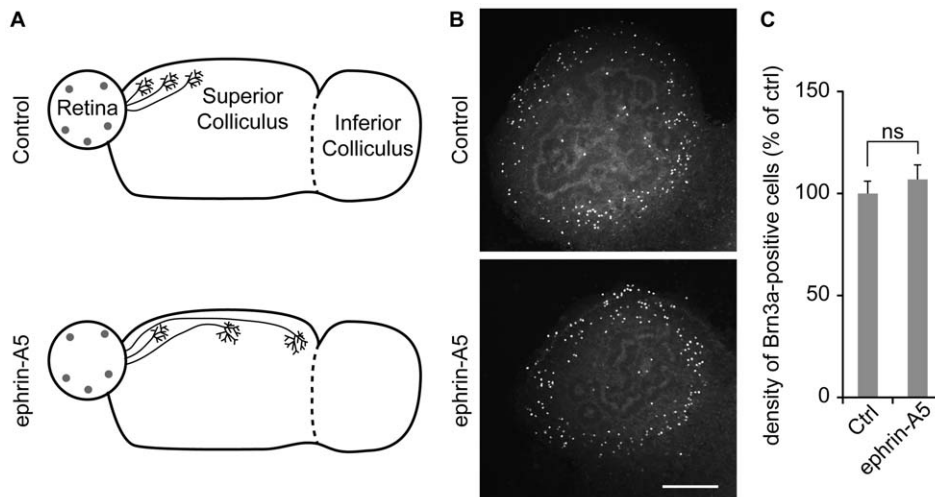


Figure 7. Blockade of ephrin-A signaling does not affect Brn3a-expressing cell number reduction. (A) Ephrin-A5 treatment prevents the retinotopic organization of axonal arbors *ex vivo*, as described in [22]. Temporal axons arborize in the rostral SC in control conditions. In contrast, overall activation of ephrin-A/EphA signaling with ephrin-A5 abolishes the preference of axons from the temporal retina for the anterior SC. Grey circles symbolize Brn3a-positive RGCs and their density is representative of the number of Brn3a-labeled cells in each condition. (B, C) The density of Brn3a-immunoreactive cells in retinal explants is not affected by application of ephrin-A5 between DIV1 and DIV12 (0.5 $\mu\text{g}/\mu\text{l}$). Error bar, s.e.m.; Scale bar 200 μm ; $n \geq 40$ cultures per condition; ns, not significant, ANOVA. doi:10.1371/journal.pone.0031105.g007

A new model to study developmental reduction of RGC population size

The evaluation of factors influencing developmental cell death *in vivo* requires the manipulation of the retina, which is usually done with injection of pharmacological agents in the eye or in the retinal targets in the brain [18]. Both manipulations are not possible before birth in mammals and recurring intravitreal injections are challenging in young pups of mice without damaging the retina and potentially affecting RGC survival, although this technique has been previously used in larger rodents like rat [8]. We describe here the use of an *ex vivo* model for the study of the developmental regulation of RGC population size, that enables pharmacological manipulations, including early developmental stages corresponding to embryonic ages. In addition, transgenic animals with lethal mutations at late embryonic stages or after birth can also be used [19], since the retina is dissected out at embryonic stages. Furthermore, it is possible to mix different genotypes of transgenic mice for the retina and its targets offering a convenient way to evaluate the respective roles of molecules in the retina or in the target cells [22]. This experimental model has been previously used to assess the development of retino-collicular topography and mimics the development of retinal projections and its dependence on ephrin-A signaling [22]. The development of retinal electrical activity follows *ex vivo* a similar time course as its maturation *in vivo* [19]. Here, we extended the repertoire of events showing close similarities in the maturation of the retina *in vivo* and *ex vivo*. Thus, the development of photoreceptors, starburst amacrine cells and RGCs follows a similar time course *in vivo* and *ex vivo*, although there is a noticeable acceleration of RGC cell death at the beginning of the culture period as previously reported [37] and which may be related to the axotomy of retinal axons that had already reached their brain target at the time when the retinal explants are dissected. Interestingly however, the number of RGCs was stable between DIV12 and DIV21, suggesting that the period of RGC cell death is closed at DIV12, which corresponds to P7 *in vivo*. This is earlier than the end of the

period of RGC cell death which is estimated at the end of the second postnatal week in mice [3]. In addition, the spatial reorganization of the different cell types within the retinal explant suggests that the laminar organization of the retina is mimicked *ex vivo*, resembling other retinal explants models *in vitro* [38,39].

Modulation of developmental reduction of RGC number by electrical activity and target availability

The massive reduction of RGC number *in vivo* is mimicked *ex vivo*. Blockade of electrical activity in the rat retina has previously been found to modulate the survival of RGCs with large scale targeting errors [11,12]. We show here that blocking electrical activity reduces the decrease in Brn3a-expressing RGCs in mouse retinal explants. These results extend the modulation of RGC population size by electrical activity to a large population of RGCs. However it should be noted that even though activity blockade effect raised the population of Brn3a neurons by 64%, this effect is fairly limited when considering the initial pool of Brn3a neurons (84% cell death in TTX, compared to 90% reduction in control conditions). Thus, most of Brn3a-positive cells are not sensitive to TTX and undergo cell death, suggesting that electrical activity is a modulator of developmental cell death but is not a major molecular pathway for reducing the RGC population size.

Electrical activity is required for competition-driven selection of surviving RGCs. The use of the retino-collicular co-culture allowed the modulation of the target size. We found that increasing the size of available SC increased the surviving RGCs between DIV4 and DIV12, corresponding to P0 and P7 respectively *in vivo*. This observation confirms previous observations indicating that reduction of SC targets decreases RGC survival [7]. Interestingly, late-born RGCs acquire target-dependent survival with a delay compared to RGCs generated earlier [40]. It will be of interest to examine whether this feature is maintained *ex vivo*, to better understand the differences between these two populations of RGCs.

Regulation of RGC number is competition-dependent but is not influenced by ephrin-A signaling

RGC developmental cell death has been suggested to favor the selective elimination of ectopic projections of retinal axons in the SC [5,11,12,18]. Ephrin-A signaling is critical for the topographic organization of retinal projections both *in vivo* and in the retino-collicular co-culture [22,33,41]. Moreover, ephrin-A signaling promotes apoptosis of neuronal progenitors in the cerebral cortex [34]. However, it is still unclear whether topographic defects in retinal projections induced by lack of ephrin-A signaling affect RGC developmental cell death [42]. We tested this hypothesis with the generation of an abnormal retino-collicular projection *ex vivo*, using ephrin-A5 to induce an overall stimulation of ephrin-A/EphA signaling. We found no change in the number of RGCs in ectopically projecting retinal explants. We conclude that the ephrin-A-dependent refinement of retinal projection does not rely on the elimination of ectopically projecting RGCs. This is in agreement with observations showing that the refinement of eye-specific domains in the visual thalamus is unaltered in mice overexpressing Bcl2, an anti-apoptotic gene increasing the number of RGCs when overexpressed [43].

The present *ex vivo* analysis showed that RGC developmental cell death is modulated by electrical activity and target size but is not dependent on ephrin-A signaling. This implies that electrical activity in the retina modulates independently RGC population size and the organization of retinal arbors in visual target fields. The effects of electrical activity on RGC cell numbers may be related to the requirement of trophic factors from the targets since neural activity modulates expression of trophic factors [44–46]. On the other hand, the activity-dependent development of retinal maps likely involves different mechanisms, as shown for the regulation of ephrin-As signaling pathway [19], and a synaptic transmission-dependent mechanism to confine projections of individual RGCs in small areas and define ipsi and contralateral domains [47–49].

Materials and Methods

Animals

Experiments were conducted in compliance with the standard ethical guidelines (European Community guidelines on the care and use of Laboratory animals and French Agriculture and Forestry Ministry guidelines for handling animals-decree 87849, license B75-05-22. Our Institute has the authorization for the use of mice without approval of specific research project). Outbred mice with a Swiss background were obtained from Janvier's animal facility (Orleans, France). β -actin-GFP and Brn3a-LacZ reporter (generous gift of Dr E. Turner) lines were obtained from local colonies. E0.5 is the day following the mating night P0 is the day of birth.

Histology

Pups were fixed by perfusion through the heart with 4% paraformaldehyde after cold anesthesia at P0, P3, and P7. The eyes were dissected out, post-fixed for 12 hours, and cryoprotected in 10% sucrose. 15 μ m thick serial sections were obtained from the frozen eyes using a cryostat. Sections were washed 1 h in PBS-0.2% gelatin and 0.25% Triton X-100, and incubated overnight at room temperature in anti-Brn3a (1/200; Abcys), anti-recoverin (1/1000; Abcys), or anti-ChAT (1/200; Chemicon-Millipore). They were washed again and incubated for 2 h at room temperature in the appropriate secondary antibody coupled to Alexa 488 (1/200; Invitrogen) or Cy3 (1/200; Jackson). Sections were finally washed in PBS and mounted in mowiol-Dabco (25 mg/ml; Sigma).

Organotypic co-cultures

Organotypic retino-collicular co-cultures were prepared as previously described [22]. Briefly, a block containing the superior and inferior colliculus was dissected out of brains from P6 pups in cold PBS-0.5% glucose, and sliced into 300 μ m-thick para-sagittal slices using a tissue chopper. Slices selected from the center of each SC were transferred on a Millicell culture insert with 0.4 μ m pore size (Millipore), and maintained in 5% CO₂ at 35°C. E15.5 embryos were obtained from pregnant OF1, β -actin-GFP or Brn3a-LacZ reporter mice. The retinas were dissected out, placed in culture medium and cut into 200 μ m² explants. Individual retinal explants were placed rostral and in contact with one, two or four SC slices, that had been cultured the day before. In the presence of more than one SC slice per retinal explant, all the slices were oriented in order to have the retinal explant placed along the rostral part of the dorsal SC. The co-culture preparations were then cultured for 4, 7, 12 or 21 days at 35°C in 5% CO₂. The culture medium used was composed of 60% basal medium eagle (BME) (Invitrogen), 20% inactivated horse serum (Invitrogen), 20% 1 \times HBSS (Invitrogen), 0.4% glucose (Invitrogen), 0.8 mM glutamine (Invitrogen) and was replaced every 2 days. For pharmacological manipulations, TTX (2.5 μ M; Euromedex) or ephrin-A5 (0.5 μ g/ml; R&D Systems) were added the day after the beginning of the culture (DIV1) and at each medium change.

Cultures were fixed for 10 minutes in 4% paraformaldehyde, with 15% sucrose at room temperature, washed 10 minutes in PBS before non specific binding was blocked with 10% fetal bovine serum in PBS, 0.1% Tween 20 (1 h) at room temperature. Primary anti-Brn3a (1/200; Absys), anti-recoverin (1/1000; Abcys), anti-ChAT (1/200; Chemicon-Millipore), or anti-GFP (1/1000; Invitrogen) antibody was diluted in the blocking solution and applied for 1 h at room temperature. The cultures were washed 10 minutes in PBS-0.1%Tween 20 and secondary antibody (goat anti-mouse coupled to Alexa 488 fluorochrome (1/200; Invitrogen) was diluted in the blocking solution and added for 1 hour at room temperature, before counterstaining with bisbenzimidazole (10 μ g/ml; Sigma). The co-culture preparations were finally washed in PBS and mounted in mowiol-Dabco (25 mg/ml; Sigma).

For β -galactosidase revelation, cultures were fixed for 10 minutes in 4% paraformaldehyde, rinsed 3 times in PBS and incubated overnight in the staining solution (5 mM K₄Fe(CN)₆, 5 mM K₃Fe(CN)₆, 2 mM MgCl₂, 1 mg/ml X-gal in PBS). The tissue was rinsed 3 times in PBS and mounted in mowiol.

Electrophysiological recordings

Extracellular recordings of the mesencephalic slice were done as previously described [19]. Briefly, cultures were placed in an interface recording chamber and superfused with an artificial cerebrospinal fluid (ACSF) containing 125 mM NaCl, 4.5 mM KCl, 2.5 mM NaHCO₃, 1 mM CaCl₂, 1 mM MgCl₂ and 10 mM D-glucose, equilibrated with 5% CO₂ in O₂. Records were made using tungsten electrodes. Data was acquired using Axoscope software (Molecular Devices) and digitized at a temporal resolution of 0.05 ms.

Data Analysis

Count of Brn3a-, recoverin- and ChAT-positive cells in the retina. The 2 sections of the retina with the largest diameter were identified and micrographs were obtained using a wide field fluorescence microscope and a 5 \times objective. Their dimensions were used to compute the total surface of the retina. The retina was approximated to a spherical cap and its area was computed

using the following formula: $S = 2\pi rh$, where r is the radius of the sphere, and h the height of the spherical cap. Micrographs of the immunostained retinas were obtained using a wide field fluorescence microscope and a $20\times$ objective. The density of Brn3a- and ChAT- positive cells (number of cells per μm^2 of retinal surface) was measured from ≥ 4 fields of the retina for each animal using the ITCN plugin of ImageJ (W. Rasband, NIH) for Brn3a-positive RGCs or manually for ChAT-positive amacrine cells, and multiplied by the computed surface to obtain an estimate of the total number of each cell type in the retina. Each recoverin-stained retinal section was manually thresholded and the area covered by immunolabeling was measured using ImageJ. The measured area was divided by the length of the retina (to measure the area/unit length) and multiplied by the computed surface of the retina to estimate the volume occupied by recoverin-positive cells in the entire retina. Statistical comparisons were performed using the Kruskal-Wallis test.

Density of Brn3a-, ChAT- and recoverin-positive cells and pyknotic profiles in retinal explants *in vitro*. Micrographs of the retinal explants were obtained using a wide field fluorescence microscope. For each explant Brn3a-, ChAT-positive cells or pyknotic profiles were manually counted in two $310\times 245\ \mu\text{m}$ fields for ≥ 10 explants per conditions. One region was chosen as the region with the highest Brn3a-expressing cells density in the peripheral zone of the explant. The other field was

the densest region in the center of the explant. The count of ChAT-positive cells was performed in two fields in the peripheral zone of the explants. Densities of Brn3a- and ChAT-positive RGCs were normalized to those obtained in parallel control cultures (DIV4 for time course experiments, free of drugs for pharmacology experiments). Densities of pyknotic profiles were normalized to the density of Brn3a-positive cells at DIV4 to give an approximation of the percentage of RGCs lost at each age. The density of recoverin staining in the retinal explant was measured after thresholding the fluorescence of the micrographs and normalized to the value obtained in parallel cultures at DIV4. Statistical comparisons were performed using ANOVA.

Acknowledgments

We thank Dr R. Miles for help with the electrophysiological recording and Dr E. Turner for the gift of the Brn3a-LacZ reporter mouse line. We are grateful to members of our lab for thoughtful discussions and to Fiona Francis and Alexandra Rebsam for critical reading of the manuscript.

Author Contributions

Conceived and designed the experiments: SV PG. Performed the experiments: SV AM. Analyzed the data: SV XN. Wrote the paper: SV PG XN.

References

- Buss RR, Sun W, Oppenheim RW (2006) Adaptive roles of programmed cell death during nervous system development. *Annu Rev Neurosci* 29: 1–35.
- Vecino E, Hernández M, García M (2004) Cell death in the developing vertebrate retina. *Int J Dev Biol* 48: 965–974.
- Young RW (1984) Cell death during differentiation of the retina in the mouse. *J Comp Neurol* 229: 362–373.
- Young RW (1985) Cell proliferation during postnatal development of the retina in the mouse. *Brain Res* 353: 229–239.
- Galli-Resta L, Ensigni M (1996) An intrinsic time limit between genesis and death of individual neurons in the developing retinal ganglion cell layer. *J Neurosci* 16: 2318–2324.
- Scheetz AJ, Williams RW, Dubin MW (1995) Severity of ganglion cell death during early postnatal development is modulated by both neuronal activity and binocular competition. *Vis Neurosci* 12: 605–610.
- Wikler KC, Kim J, Windrem MS, Finlay BL (1986) Control of cell number in the developing visual system. II. Effects of partial tectal ablation. *Brain Res* 393: 11–21.
- Cui Q, Harvey AR (1995) At least two mechanisms are involved in the death of retinal ganglion cells following target ablation in neonatal rats. *J Neurosci* 15: 8143–8155.
- Ma YT, Hsieh T, Forbes ME, Johnson JE, Frost DO (1998) BDNF injected into the superior colliculus reduces developmental retinal ganglion cell death. *J Neurosci* 18: 2097–2107.
- Harvey AR, Robertson D (1992) Time-course and extent of retinal ganglion cell death following ablation of the superior colliculus in neonatal rats. *J Comp Neurol* 325: 83–94.
- Fawcett JW, O'Leary DD, Cowan WM (1984) Activity and the control of ganglion cell death in the rat retina. *Proc Natl Acad Sci USA* 81: 5589–5593.
- O'Leary DD, Fawcett JW, Cowan WM (1986) Topographic targeting errors in the retinocollicular projection and their elimination by selective ganglion cell death. *J Neurosci* 6: 3692–3705.
- Siminoff R, Schwassmann HO, Kruger L (1966) An electrophysiological study of the visual projection to the superior colliculus of the rat. *J Comp Neurol* 127: 435–444.
- Eysel UT, Wolfhard U (1983) Morphological fine tuning of retinotopy within the cat lateral geniculate nucleus. *Neurosci Lett* 39: 15–20.
- Simon DK, O'Leary DD (1990) Limited topographic specificity in the targeting and branching of mammalian retinal axons. *Dev Biol* 137: 125–134.
- Simon DK, O'Leary DD (1992) Development of topographic order in the mammalian retinocollicular projection. *J Neurosci* 12: 1212–1232.
- Sachs GM, Jacobson M, Caviness VS (1986) Postnatal changes in arborization patterns of murine retinocollicular axons. *J Comp Neurol* 246: 395–408.
- O'Leary DD, Crespo D, Fawcett JW, Cowan WM (1986) The effect of intraocular tetrodotoxin on the postnatal reduction in the numbers of optic nerve axons in the rat. *Brain Res* 395: 96–103.
- Nicol X, Voyatzis S, Muzerelle A, Narboux-Nême N, Südhof TC, et al. (2007) cAMP oscillations and retinal activity are permissive for ephrin signaling during the establishment of the retinotopic map. *Nat Neurosci* 10: 340–347.
- Dräger UC, Olsen JF (1980) Origins of crossed and uncrossed retinal projections in pigmented and albino mice. *J Comp Neurol* 191: 383–412.
- Quina LA, Pak W, Lanier J, Banwait P, Gratwick K, et al. (2005) Brn3a-expressing retinal ganglion cells project specifically to thalamocortical and collicular visual pathways. *J Neurosci* 25: 11595–11604.
- Nicol X, Muzerelle A, Rio JP, Métin C, Gaspar P (2006) Requirement of adenylate cyclase 1 for the ephrin-A5-dependent retraction of exuberant retinal axons. *J Neurosci* 26: 862–872.
- Dizhoor AM, Ray S, Kumar S, Niemi G, Spencer M, et al. (1991) Recoverin: a calcium sensitive activator of retinal rod guanylate cyclase. *Science* 251: 915–918.
- Yoshida K, Watanabe D, Ishikane H, Tachibana M, Pastan I, et al. (2001) A key role of starburst amacrine cells in originating retinal directional selectivity and optokinetic eye movement. *Neuron* 30: 771–780.
- Feller MB, Wellis DP, Stellwagen D, Werblin FS, Shatz CJ (1996) Requirement for cholinergic synaptic transmission in the propagation of spontaneous retinal waves. *Science* 272: 1182–1187.
- Crespo D, O'Leary DD, Cowan WM (1985) Changes in the numbers of optic nerve fibers during late prenatal and postnatal development in the albino rat. *Brain Res* 351: 129–134.
- Perry VH, Henderson Z, Linden R (1983) Postnatal changes in retinal ganglion cell and optic axon populations in the pigmented rat. *J Comp Neurol* 219: 356–368.
- Voyvodic JT, Burne JF, Raff MC (1995) Quantification of normal cell death in the rat retina: implications for clone composition in cell lineage analysis. *Eur J Neurosci* 7: 2469–2478.
- Hadjantonakis AK, Gertsenstein M, Ikawa M, Okabe M, Nagy A (1998) Generating green fluorescent mice by germline transmission of green fluorescent ES cells. *Mech Dev* 76: 79–90.
- Eng SR, Gratwick K, Rhee JM, Fedtsova N, Gan L, et al. (2001) Defects in Sensory Axon Growth Precede Neuronal Death in Brn3a-Deficient Mice. *J Neurosci* 21: 541–549.
- Thompson I, Holt C (1989) Effects of intraocular tetrodotoxin on the development of the retinocollicular pathway in the Syrian hamster. *J Comp Neurol* 282: 371–388.
- Galli-Resta L, Ensigni M, Fusco E, Gravina A, Margheriti B (1993) Afferent spontaneous electrical activity promotes the survival of target cells in the developing retinotectal system of the rat. *J Neurosci* 13: 243–250.
- Feldheim DA, Vanderhaeghen P, Hansen MJ, Frisén J, Lu Q, et al. (1998) Topographic guidance labels in a sensory projection to the forebrain. *Neuron* 21: 1303–1313.
- Depaape V, Suarez-Gonzalez N, Dufour A, Passante L, Gorski JA, et al. (2005) Ephrin signalling controls brain size by regulating apoptosis of neural progenitors. *Nature* 435: 1244–1250.
- Farah MH, Easter SS, Jr. (2005) Cell birth and death in the mouse retinal ganglion cell layer. *J Comp Neurol* 489: 120–134.
- Jeon CJ, Strettoi E, Masland RH (1998) The major cell populations of the mouse retina. *J Neurosci* 18: 8936–8946.

37. Meyer-Franke A, Kaplan MR, Pflieger FW, Barres BA (1995) Characterization of the signaling interactions that promote the survival and growth of developing retinal ganglion cells in culture. *Neuron* 15: 805–819.
38. McLoon LK, McLoon SC, Lund RD (1981) Cultured embryonic retinae transplanted to rat brain: differentiation and formation of projections to host superior colliculus. *Brain Res* 226: 15–31.
39. Bytyqi AH, Bachmann G, Rieke M, Paraoanu LE, Layer PG (2007) Cell-by-cell reconstruction in reagggregates from neonatal gerbil retina begins from the inner retina and is promoted by retinal pigmented epithelium. *Eur J Neurosci* 26: 1560–1574.
40. Dallimore EJ, Park KK, Pollett MA, Taylor JSH, Harvey AR (2010) The life, death and regenerative ability of immature and mature rat retinal ganglion cells are influenced by their birthdate. *Exp Neurol* 225: 353–365.
41. Drescher U, Kremoser C, Handwerker C, Lösinger J, Noda M, et al. (1995) In vitro guidance of retinal ganglion cell axons by RAGS, a 25 kDa tectal protein related to ligands for Eph receptor tyrosine kinases. *Cell* 82: 359–370.
42. Haustead DJ, Lukehurst SS, Clutton GT, Bartlett CA, Dunlop SA, et al. (2008) Functional topography and integration of the contralateral and ipsilateral retinocollicular projections of ephrin-A^{-/-} mice. *J Neurosci* 28: 7376–7386.
43. Yakura T, Fukuda Y, Sawai H (2002) Effect of Bcl-2 overexpression on establishment of ipsilateral retinocollicular projection in mice. *Neuroscience* 110: 667–673.
44. Spalding KL, Rush RA, Harvey AR (2004) Target-derived and locally derived neurotrophins support retinal ganglion cell survival in the neonatal rat retina. *J Neurobiol* 60: 319–327.
45. Spalding KL, Cui Q, Harvey AR (2005) Retinal ganglion cell neurotrophin receptor levels and trophic requirements following target ablation in the neonatal rat. *Neuroscience* 131: 387–395.
46. Frade JM, Bovolenta P, Martínez-Morales JR, Arribas A, Barbas JA, et al. (1997) Control of early cell death by BDNF in the chick retina. *Development* 124: 3313–3320.
47. Dhande OS, Hua EW, Guh E, Yeh J, Bhatt S, et al. (2011) Development of single retinofugal axon arbors in normal and $\beta 2$ knock-out mice. *J Neurosci* 31: 3384–3399.
48. Rossi FM, Pizzorusso T, Porciatti V, Marubio LM, Maffei L, et al. (2001) Requirement of the nicotinic acetylcholine receptor $\beta 2$ subunit for the anatomical and functional development of the visual system. *Proc Natl Acad Sci U S A* 98: 6453–6458.
49. Grubb MS, Rossi FM, Changeux J-P, Thompson ID (2003) Abnormal Functional Organization in the Dorsal Lateral Geniculate Nucleus of Mice Lacking the $\beta 2$ Subunit of the Nicotinic Acetylcholine Receptor. *Neuron* 40: 1161–1172.